First-Principles Calculations of Angle-Resolved and Spin-Resolved Photoemission Spectra of Cr(110) Surfaces at the $2p$-$3d$ Cr Resonance

Fabiana Da Pieve[1] and Peter Krüger[2]

[1]*ALGC, Vrije Universiteit Brussel, Pleinlaan 2, 1050 Brussels, Belgium*

[2]*ICB, UMR 6303 CNRS, Université de Bourgogne, F-21078 Dijon, France*

(Received 30 August 2012; published 18 March 2013)

A first principles approach for spin- and angle-resolved resonant photoemission is developed within multiple scattering theory and applied to a Cr(110) surface at the $2p$-$3d$ resonance. The resonant photocurrent from this nonferromagnetic system is found to be strongly spin polarized by circularly polarized light, in agreement with experiments on antiferromagnetic and magnetically disordered systems. By comparing the antiferromagnetic and Pauli-paramagnetic phases of Cr, we explicitly show that the spin polarization of the photocurrent is independent of the existence of local magnetic moments, solving a long-standing debate on the origin of such polarization. New spin polarization effects are predicted for the paramagnetic phase even with unpolarized light, opening new directions for full mapping of spin interactions in macroscopically nonmagnetic or nanostructured systems.

DOI: 10.1103/PhysRevLett.110.127401 PACS numbers: 78.20.Bh, 78.20.Ls, 78.70.−g, 79.60.−i

In recent years, the theoretical description of absorption or photoemission spectroscopy in the x-ray region has been boosted by the merge of density functional theory (DFT) with many body approaches such as dynamical mean field theory [1,2], many body perturbation theory [3–5], and by the development of time-dependent DFT [6]. However, second order processes, like resonant inelastic x-ray scattering and resonant photoemission (RPES), remain a major challenge for theory. For RPES, existing approaches are semiempirical [7–10], based on a well-defined two-holes final state and on small clusters, and thus do not take into account the delocalization of intermediate states, the band structure of the system, and multiple scattering effects in the propagation of photoelectrons.

The huge experimental output from RPES on correlated materials [7,11–16] and the intriguing quest for a determination of local magnetic properties put forward by pioneering experiments [14–16] call for advancements in the theoretical description of this spectroscopy. In experiments on CuO and Ni, it was shown that the RPES photocurrent with circular polarized light is spin polarized in antiferromagnets [14,15] and Curie paramagnets [16]. It was claimed that a specific combination of spin-resolved spectra provides a direct measure of the local magnetic moments [14–16]. The issue is of fundamental importance in the search for a tool to access the local magnetic properties in antiferromagnetic, magnetically disordered and/or nanostructured systems at their crossover with the transition temperature. The interpretation was however rejected on the basis of symmetry analysis [17], but explicit calculations predicting the line shape and intensity of such a fundamental signal are still lacking and remain highly desirable.

In this Letter, we present the first *ab initio* method for RPES in solids, based on a combined formulation within the real space multiple scattering (RSMS) approach [18,19] and DFT, and its application to Cr(110) at the $2p$-$3d$ resonance. By comparing the antiferromagnetic (AFM) and Pauli-paramagnetic (PM) phase of Cr, we solve the long-standing debate about the possibility to determine local magnetic moments in macroscopically nonmagnetic systems by means of spin-resolved RPES with circular polarized light. New interesting effects in the PM phase by unpolarized light suggest that other mechanisms are active and could be exploited for mapping the origin of the different spin polarization (SP) components in paramagnets and magnetically disordered systems.

Theoretical formulation.—The cross section for valence band photoemission to a final state $|\underline{v}, k\rangle$, where $\underline{v}$ denotes a valence band hole and k a photoelectron state, is given by

$$I(\omega, q, k) = \sum_{v} |T_{kv}(\omega, q)|^2 \delta(\epsilon_k - \epsilon_v - \hbar\omega),$$

where $\hbar\omega$ and q are the photon energy and polarization. Here the independent particle approximation has been assumed (i.e., all many-electron eigenstates are single Slater determinants corresponding to the same effective one-electron Hamiltonian). According to the Heisenberg-Kramers formula [20], the transition matrix element $T_{kv}(\omega, q)$ is the sum of a direct and a resonant term. In the latter, photon absorption leads to an intermediate state $|\underline{c}, u\rangle$, with a core hole ($\underline{c}$) and an electron in a formerly unoccupied state $|u\rangle$, which decays to the final state $|\underline{v}, k\rangle$ through a participator Auger process [20,21]. To lowest order in the autoionization process, the transition matrix element is given by

$$T_{kv}(\omega, q) = \langle k|D_q|v\rangle + \sum_{cu} \frac{\langle kc|V(|vu\rangle - |uv\rangle)}{\hbar\omega + \epsilon_c - \epsilon_u - i\Gamma} \langle u|D_q|c\rangle, \quad (1)$$

where D_q is the dipole operator, V the Coulomb operator, and Γ the width of the intermediate state. Spectator Auger decay leads to different, namely, two-hole final states and is not considered here. Participator and spectator channels can in principle be separated experimentally by using a photon bandwidth smaller than the core-hole lifetime, as they show different photon energy dependence (linear for the participator, and no photon energy dependence for the spectator). Here we focus on the physical effects at the origin of spin polarization and dichroism as well as their directional dependence in the "pure" participator channel.

The RPES intensity can be written in a compact form as

$$I(\omega, q, k) = \sum_{ijLL'\sigma} M^{\omega,q}_{iL\sigma}(k) I^{ij}_{LL'}(\epsilon_v, \sigma) M^{\omega,q}_{jL'\sigma}(k)^*.$$

Here, i, j label atomic sites, $L \equiv (lm)$ angular momentum, and σ spin quantum numbers. $\epsilon_v = \epsilon_k - \hbar\omega$ is the energy of the valence hole. The quantity $I^{ij}_{LL'} \equiv -\frac{1}{2i\pi}(\tau - \tau^\dagger)^{ij}_{LL'}$ is the essentially imaginary part of the scattering path operator. It comes from the simplification of the sum over delocalized valence states through the so-called optical theorem in RSMS [22] and it contains the band structure information. The matrix elements $M^{\omega,q}_{iL\sigma}(k)$ are given by

$$M^{\omega,q}_{iL\sigma}(k) = \sum_{jL'} B^*_{jL'}(k) A_{jL',iL}(\epsilon_k\sigma_k, \epsilon_v\sigma).$$

The $B_{jL'}(k)$ are the key quantities in the RSMS approach and represent the multiple scattering amplitudes of the continuum state $k \equiv (\mathbf{k}\sigma_k)$ [22]. The matrix elements $A_{jL',iL}(\epsilon_k\sigma_k, \epsilon_v\sigma)$ are given by the sum of the direct radiative process (A^D), the resonant process with direct Coulomb decay (A^C), and the resonant process with the exchange decay (A^X), see Eq. (1). A^D and A^C are site- and spin-diagonal ($\sim \delta_{ij}\delta_{\sigma_k\sigma}$). We have

$$A^D = \langle i\epsilon_k L'\sigma | D_q | i\epsilon_v L\sigma\rangle$$

$$A^C = -\sum_{j'cL_uL'_u\sigma_u} \int_{E_F} d\epsilon_u \frac{I^{j'j'}_{L_uL'_u}(\epsilon_u\sigma_u)}{\hbar\omega + \epsilon_c - \epsilon_u - i\Gamma} \times \langle i\epsilon_k L'\sigma, j'c|V|i\epsilon_v L\sigma, j'\epsilon_u L_u\sigma_u\rangle \times \langle j'\epsilon_u L'_u\sigma_u|D|j'c\rangle$$

$$A^X = \sum_{cL_uL'_u} \int_{E_F} d\epsilon_u \frac{I^{ji}_{L_uL'_u}(\epsilon_u\sigma_k)}{\hbar\omega + \epsilon_c - \epsilon_u - i\Gamma} \times \langle j\epsilon_k L_k\sigma_k, ic|V|j\epsilon_u L_u\sigma_k, i\epsilon_v L\sigma\rangle\langle i\epsilon_u L'_u\sigma_k|D|ic\rangle.$$

The sums over unoccupied states u have been again simplified through the optical theorem. The exchange term A^X is not strictly site-diagonal because of the nonlocality of the exchange interaction together with the delocalized nature of the states u. In the RSMS approach the Coulomb matrix elements $\langle kc|V|vu\rangle$ and $\langle kc|V|uv\rangle$ can be exactly developed in one- and two-center terms. In metallic Cr, the Coulomb interaction is strongly screened. As a result, two-center terms are by at least 1 order of magnitude smaller than the one-center terms [23] and have been neglected here. In general, the $2p$-$3d$ excited intermediate states might display excitonic effects, which could be taken account for with a Bethe-Salpeter description [3,5]. For Cr metal, these effects are quite small because of the large $3d$ band width (~ 7 eV) and efficient metallic screening of the core hole by nearly free $4sp$ electrons, and thus neglected here.

Photoemission spectra from Cr(110) are calculated in RSMS with a cluster of 151 atoms [see Fig. 1(a)] and self-consistent spin-polarized potentials, obtained by a scalar relativistic linear muffin tin orbital (LMTO) [24] calculation for bulk Cr in the local spin density approximation. Except for the $2p$ core level, all states entering the RPES calculation are developed in RSMS. The $2p$ orbital is obtained by solving the scalar relativistic Schrödinger equation with self-consistent spin-polarized LMTO potentials. The $2p_{3/2}$ spin-orbit coupled states are then constructed using standard angular momentum algebra and the spin-orbit coupling constant is taken from an atomic calculation [25]. We consider the AFM order of CsCl-type, which is a good approximation to the true spin density wave (SDW) ground state of Cr. The calculated magnetic moment is $0.74\mu_B$, in reasonable agreement with experiment ($0.62\mu_B$). At the (110) surface, the transverse SDW propagates along [100] or [010] [26]. Therefore, we take

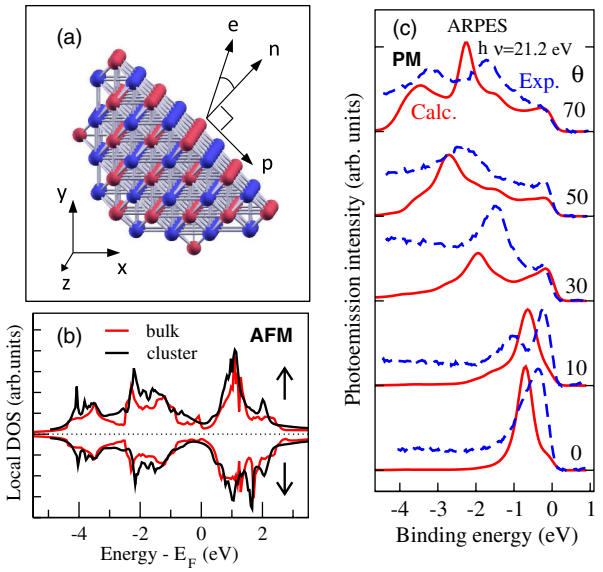

FIG. 1 (color online). (a) Cr(110) cluster used in the RSMS calculations. The two magnetic sublattices of the AFM state are in red and blue. (b) DOS in the AFM phase for a bulk atom (LMTO) and a central atom in the cluster (RSMS). (c) ARPES spectra from Cr(110) along the ⟨001⟩ azimuth for different polar angles θ with respect to the surface normal. Unpolarized light along the [001] axis was considered. Experimental data from Ref. [28].

$\mathbf{e}_z = [001]$ as the magnetization and spin-quantization axis throughout this Letter. We also consider the Pauli PM state, corresponding to a nonmagnetic calculation. Spin orbit (SO) coupling of the valence and continuum states is neglected (it is as small as 0.03 eV for Cr-3d [27]).

Results.—The electronic structure of Cr(110) is well accounted for in the RSMS approach as can be seen from the comparison between the local density of states (DOS) of a Cr atom in the cluster and of bulk Cr [Fig. 1(b)]. Nonresonant angle-resolved photoemission spectra (ARPES) are shown in Fig. 1(c). Differences with respect to experiments [28] are expected as our approach does not contain local many-body interactions and layer-dependent potentials, which could play a role for a quantitative description of the peak renormalization and dispersion behavior of the energetic structures [29]. However, the main features of the experimental spectra are reproduced in the calculation, confirming that RSMS provides a reasonably good description of valence band photoemission from metals as previously shown for Cu(111) [22].

Spin-resolved, angle integrated PES and RPES spectra are shown in Fig. 2 for the AFM phase and several photon energies across the L_3-edge absorption threshold. Left circular polarized light incident along the magnetization axis [001] is considered. In this "parallel" geometry, right polarized light produces the same spectra as left polarized light but with up and down spin exchanged. The maximum peak intensity as a function of photon energy is plotted in Fig. 2(b) and shows the expected Fano profile. The first photon energy (551.0 eV) is too low to excite the core electron and so only direct PES is possible. When the photon energy is raised to 552.4 eV, just below the absorption edge, direct and resonant processes interfere destructively, giving rise to the dip in the Fano profile. Strong resonant enhancement is observed between 552 and 554.5 eV (see, e.g., the spectrum for 554.4 eV), which corresponds to transitions from the $2p_{3/2}$ level into the unoccupied Cr 3d band. At $h\nu = 585.1$ eV, well above threshold, the resonant spectrum goes back to the nonresonant one.

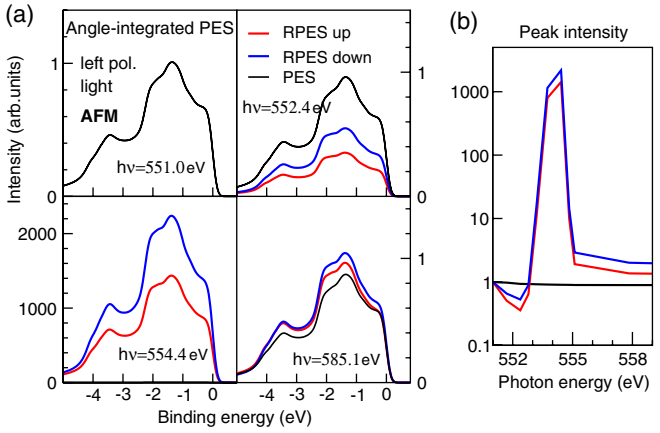

FIG. 2 (color online). (a) Spin-resolved, angle integrated RPES and PES spectra of AFM Cr(110) with left circular polarized light incoming along the spin quantization axis [001] and photon energies across the L_3-edge resonance. A Gaussian broadening of 0.27 eV FWHM was applied. Note the different intensity scale for $h\nu = 554.4$ eV. In PES, spin-up and spin-down intensities are equal in all cases. (b) Maximum peak intensity as a function of photon energy.

The direct PES signal is non-spin-polarized as expected for the AFM phase. Appreciable spin polarization is, however, found in RPES. This effect is here obtained for the first time through first-principles calculations, and confirms the experimental finding in CuO [14], that in AFM systems RPES at the $2p_{3/2}$-3d resonance is spin-polarized when circular polarized light is used.

We now turn to angle- and spin-resolved spectra at maximum resonance ($h\nu = 554.4$ eV), focusing on their four "fundamental" combinations (and their relation to local magnetic properties), constructed by different choices of photoelectron spin ($\uparrow$, $\downarrow$) and light helicity ($+$, $-$) $\equiv$ (left, right):

$$\begin{aligned}
\text{tot} &\equiv (\uparrow +) + (\uparrow -) + (\downarrow +) + (\downarrow -) \quad \text{(total)} \\
\text{spr} &\equiv (\uparrow +) + (\uparrow -) - (\downarrow +) - (\downarrow -) \quad \text{(spin resolved)} \\
\text{dic} &\equiv (\uparrow +) - (\uparrow -) + (\downarrow +) - (\downarrow -) \quad \text{(dichroic)} \\
\text{mix} &\equiv (\uparrow +) - (\uparrow -) - (\downarrow +) + (\downarrow -) \quad \text{(mixed).}
\end{aligned}$$

The "mixed" spectrum was the one considered in Refs. [14,16] and claimed to be sensitive to local magnetic moments in nonferromagnetic samples.

The normal emission RPES spectra [Figs. 3(a) and 3(b)] (total spectra) for parallel geometry consist of a single peak at 0.8–0.9 eV binding energy, very similar to the low energy nonresonant spectrum in Fig. 1(c) ($\theta = 0°$). AFM and PM spectra are almost identical except for a small shift of $\sim$0.1 eV, which reflects the small exchange splitting of the AFM Cr-3d bands. The dichroic (dic) and spin-resolved (spr) signals vanish for both the PM and AFM phase, as expected since the system is globally nonmagnetic in both cases, and the setup is nonchiral.

However, the mixed signal is nonzero with a large amplitude ($\sim 1/3$ of total), in agreement with the experimental results in AFM CuO [14]. Surprisingly, we find a nonzero mixed signal not only in the AFM, but also in the PM phase with nearly the same intensity. It is important to note that we are not considering a Curie paramagnet (such as Ni above T_C [16]) with disordered and/or fluctuating magnetic moments, but a Pauli PM state, where the magnetization is strictly zero in all points of space. Therefore, our finding that the mixed signal is essentially unchanged when going from the AFM to the PM state unambiguously proves that it is unrelated to local magnetic moments, in contrast to the interpretation in Refs. [14,16].

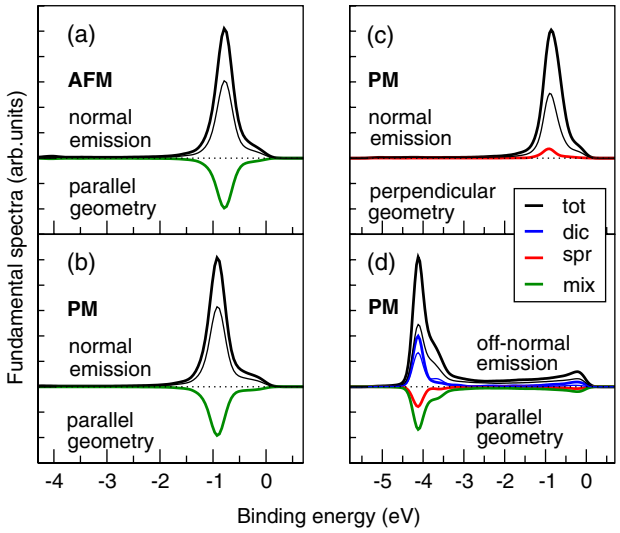

FIG. 3 (color online). Angle-resolved fundamental spectra of Cr(110). RPES as thick lines for $h\nu = 544.4$ eV. Normal (i.e., nonresonant) ARPES as thin lines, intensity × 1000. All spectra are rescaled to the equal peak height of RPES—tot. (a) AFM, (b)–(d) PM phase. (a)–(c) Normal emission. (d) Emission in the xy plane, off-normal by 23° [vector **e** in Fig. 1(a)]. Light incidence parallel [(a),(b),(d)] or perpendicular (c) to spin-quantization axis $\mathbf{e}_z$. Light vector in (c) is shown as **p** in Fig. 1(a).

Rather than being of magnetic origin, the nonzero mixed signal is in fact induced by angular momentum transfer from the light helicity to the electron spin via the SO in the core shell together with a strong exchange effect in the decay process. To see this, consider light with left (+) helicity and a nonmagnetic ground state. The $2p_{3/2}$-$3d$ optical transition has a larger amplitude for spin-up than for spin-down electrons because of the dominantly parallel alignment of spin and orbit in $2p_{3/2}$. For example, for an empty or spherically symmetric $3d$ shell the intensity ratio is 5:3. Consider now a spin-up electron transition. The RPES intermediate state has one extra spin-up electron in the $3d$ shell (denoted $u\uparrow$) and a $2p$ hole of dominant spin-up character. This state decays through Coulomb interaction to the photoemission final state with one $3d$ hole and the photoelectron. The direct Coulomb matrix elements is of the form $\langle k\sigma, c\uparrow|V|v\sigma, u\uparrow\rangle$ which is independent of the photoelectron spin σ. So the direct decay alone would lead to a spin-balanced photocurrent. For the exchange decay, the matrix element is $\langle k\sigma, c\uparrow|V|u\uparrow, v\sigma\rangle \sim \delta(\sigma,\uparrow)$. This is roughly as a large as the direct Coulomb term for spin-up electrons (the radial matrix elements are exactly the same) but it is zero for spin-down electrons. Since the exchange matrix elements are subtracted from the direct terms in Eq. (1), the transition probability for spin-up electron emission is strongly reduced by the exchange process. This shows that a core-valence transition of a spin-up electron leads, through autoionization, to a strongly spin-polarized photocurrent with a majority of spin-down electrons. As mentioned before, left circular polarized light promotes dominantly spin-up electrons in the $2p_{3/2}$-$3d$ transition. Therefore it produces a majority of spin-down photoelectrons. Under the assumption of complete cancellation between direct Coulomb and exchange matrix elements for parallel spins and by neglecting the direct valence photoemission, the ratio of spin-down to spin-up photoelectrons is 5:3, which corresponds to a spin polarization (ratio of mixed over total signal) of $-1/4$. In angle-integrated RPES at maximum resonance [Fig. 2(a), $h\nu = 554.4$ eV] we find a SP of -0.21, in good agreement with such model estimation. These values also agree well with the measured spin polarization in CuO [14] and Ni [16], which is 10%–40%, depending on binding energy. Our findings clarify the physical mechanism inducing the presence of the mixed signal in both phases, and point to a critical reexamination of experimental observations.

Interestingly, we find that, contrary to what obtained in the previous set up, it is actually possible to obtain a finite spin-resolved (spr) signal in the PM phase even with unpolarized light, if appropriate geometrical conditions are adopted. In each of these conditions, the signal can be associated to a SP originated by specific active mechanisms. In Fig. 3(c), normal emission spectra are shown for light incident along $[1\bar{1}0]$, i.e., *perpendicular* to the spin-quantization axis $\mathbf{s} = \mathbf{e}_z$ (perpendicular geometry). As before, the dichroic signal is zero, as light incidence (**p**) and electron emission vector (**n**) lie in a mirror plane of the surface] see Fig. 1(a)]. However, the setup (including spin resolution) is chiral, since the three vectors **p**, **n**, and **s** form a right-handed frame. Thus SO-induced SP cannot be ruled out by symmetry and a small, positive SP (in this case transverse to the scattering plane) is indeed observed in RPES, even for unpolarized light. A similar SP from PM surfaces for unpolarized light was theoretically predicted in direct PES [30] in a relativistic approach and confirmed by experiments [31,32]. It was ascribed to broken symmetry due to the off-normal light incidence together with SO in the initial states and phase shift differences. We do not observe this effect in nonresonant PES since the SO coupling in the Cr $3d$ valence states is very weak and neglected here. However, for RPES, such SP has to be related to the dynamical SP studied in atomic physics, which is known to be related to phase shift differences in the final outgoing waves, and to be generally small [33,34]. Our result confirms that such SP exists for an atom embedded in a solid, i.e., that it does not vanish because of multiple scattering effects.

A spin resolved signal in the PM phase is also present for parallel geometry with off normal emission [Fig. 3(d)]. In this case, the system composed by the surface, light incidence (along $\mathbf{e}_z$), and electron emission vector, is chiral. Therefore a dichroic signal is observed even in nonresonant PES, known as circular dichroism in angular distribution [35]. In RPES, the angular momentum of the

photon is partly transferred to the electron spin through the SO coupling in the $2p$ shell, leading to nonzero intensity also for spin-resolved and mixed signals. The spin polarization is negative; i.e., photoelectrons are mainly polarized antiparallel to their emission direction, because of the exchange process in the autoionization decay. This finding suggests a Fano-like effect in resonant processes for off-normal emission directions, which could be well studied along the same lines as direct PES on paramagnets [36].

In conclusion, we have presented a first-principles approach for RPES in solids and its application to Cr(110). By comparing Pauli PM and AFM states, we have shown that the mixed signal is essentially independent of local magnetic properties and we have clarified its origin: contrary to previous interpretations, this effect is induced by an angular momentum transfer from the photon to the electron spin, through SO coupling in the core level and the exchange process in the autoionization decay. Our results show that caution must be taken in linking the spin-polarized or mixed signal to local magnetic moments, all the more so as the photoelectron spin may have components along and across the light helicity. New effects in the SP suggest that a mapping of spin interactions in paramagnets and disordered magnetic structures could be obtained via full tomography experiments at the core resonances even with unpolarized light.

[1] O. Šipr, J. Minár, A. Scherz, H. Wende, and H. Ebert, Phys. Rev. B **84**, 115102 (2011).

[2] J. Braun, J. Minár, H. Ebert, M. I. Katsnelson, and A. I. Lichtenstein, Phys. Rev. Lett. **97**, 227601 (2006).

[3] W. Olovsson, I. Tanaka, T. Mizoguchi, G. Radtke, P. Puschnig, and C. Ambrosch-Draxl, Phys. Rev. B **83**, 195206 (2011).

[4] J. Vinson, J. J. Rehr, J. J. Kas, and E. L. Shirley, Phys. Rev. B **83**, 115106 (2011).

[5] R. Laskowski and P. Blaha, Phys. Rev. B **82**, 205104 (2010).

[6] O. Bunau and Y. Joly, Phys. Rev. B **85**, 155121 (2012).

[7] S. R. Mishra, T. R. Cummins, G. D. Waddill, W. J. Gammon, G. van der Laan, K. W. Goodman, and J. G. Tobin, Phys. Rev. Lett. **81**, 1306 (1998).

[8] C. F. Chang, D. J. Huang, A. Tanaka, G. Y. Guo, S. C. Chung, S.-T. Kao, S. G. Shyu, and C. T. Chen, Phys. Rev. B **71**, 052407 (2005).

[9] O. Tjernberg, G. Chiaia, U. O. Karlsson, and F. M. F. de Groot, J. Phys. Condens. Matter **9**, 9863 (1997).

[10] H. Ogasawara, A. Kotani, P. Le Fèvre, D. Chandresris, and H. Magnan, Phys. Rev. B **62**, 7970 (2000).

[11] M. Morscher, F. Nolting, T. Brugger, and T. Greber, Phys. Rev. B **84**, 140406(R) (2011).

[12] M. C. Richter, J.-M. Mariot, O. Heckmann, L. Kjeldgaard, B. S. Mun, C. S. Fadley, U. Lüders, J.-F. Bobo, P. De Padova, A. Taleb-Ibrahimi, and K. Hricovini, Eur. Phys. J. Special Topics **169**, 175 (2009).

[13] T. Ohtsuki, A. Chainani, R. Eguchi, M. Matsunami, Y. Takata, M. Taguchi, Y. Nishino, K. Tamasaku, M. Yabashi, T. Ishikawa, M. Oura, Y. Senba, H. Ohashi, and S. Shin, Phys. Rev. Lett. **106**, 047602 (2011).

[14] L. H. Tjeng, B. Sinkovic, N. B. Brookes, J. B. Goedkoop, R. Hesper, E. Pellegrin, F. M. F. de Groot, S. Altieri, S. L. Hulbert, E. Shekel, and G. A. Sawatzky, Phys. Rev. Lett. **78**, 1126 (1997).

[15] L. H. Tjeng, N. B. Brookes, and B. Sinkovic, J. Electron Spectrosc. Relat. Phenom. **117–118**, 189 (2001).

[16] B. Sinkovic, L. H. Tjeng, N. B. Brookes, J. B. Goedkoop, R. Hesper, E. Pellegrin, F. M. F. de Groot, S. Altieri, S. L. Hulbert, E. Shekel, and G. A. Sawatzky, Phys. Rev. Lett. **79**, 3510 (1997).

[17] G. van der Laan, Phys. Rev. Lett. **81**, 733 (1998).

[18] J. J. Rehr and R. C. Albers, Rev. Mod. Phys. **72**, 621 (2000).

[19] D. Sébilleau, R. Gunnella, Z.-Y. Wu, S. Di Matteo, and C. R. Natoli, J. Phys. Condens. Matter **18**, R175 (2006).

[20] A. Tanaka and T. Jo, J. Phys. Soc. Jpn. **63**, 2788 (1994).

[21] C. Janowitz, R. Manzke, M. Skibowski, Y. Takeda, Y. Miyamoto, and K. Cho, Surf. Sci. Lett. **275**, L669 (1992).

[22] P. Krüger, F. Da Pieve, and J. Osterwalder, Phys. Rev. B **83**, 115437 (2011).

[23] For nearest-neighbor (NN) two-center Coulomb terms, the average electron distance equals the NN distance d. For the one-center terms, the average distance is about $d/2$. Here it is even smaller because of the strong localization of the core orbital near the nucleus. The screened Coulomb interaction is $\exp(-r/\lambda)/r$, where λ is the screening length. The ratio between NN and on-site terms is therefore about $\chi = \exp(-d/2/\lambda)/2$. Using Thomas-Fermi theory and taking one nearly free electron ($4s$) for Cr, we get $\lambda = 0.55$ Å and $\chi = 0.052$, i.e., NN Coulomb terms are by a factor of 20 smaller than on-site terms. Further than NN, terms are obviously even much smaller.

[24] O. K. Andersen, Phys. Rev. B **12**, 3060 (1975).

[25] R. D. Cowan, *The Theory of Atomic Structure and Spectra* (University of California Press, Berkeley, 1981).

[26] K.-F. Braun, S. Fölsch, G. Meyer, and K.-H. Rieder, Phys. Rev. Lett. **85**, 3500 (2000).

[27] G. van der Laan and B. T. Thole, Phys. Rev. B **43**, 13401 (1991).

[28] P. E. S. Persson and L. I. Johansson, Phys. Rev. B **34**, 2284 (1986).

[29] J. Sànchez-Barriga *et al.*, Phys. Rev. B **85**, 205109 (2012).

[30] E. Tamura and R. Feder, Europhys. Lett. **16**, 695 (1991).

[31] J. Kirschner, Appl. Phys. A **44**, 3 (1987).

[32] N. Irmer, R. David, B. Schmiedeskamp, and U. Heinzmann, Phys. Rev. B **45**, 3849 (1992).

[33] U. Hergenhahn and U. Becker, J. Electron Spectrosc. Relat. Phenom. **76**, 225 (1995).

[34] B. Lohmann, J. Phys. B **32**, L643 (1999).

[35] J. Henk, A. M. N. Niklasson, and B. Johansson, Phys. Rev. B **59**, 13986 (1999).

[36] J. Minár, H. Ebert, G. Ghiringhelli, O. Tjernberg, N. B. Brookes, and L. H. Tjeng, Phys. Rev. B **63**, 144421 (2001).